A novel tracking tool for the analysis of plant-root tip movements

A novel tracking tool for the analysis of plant-root tip movements

A Russino[1,4], A Ascrizzi[1,2,4], L Popova[1,2], A Tonazzini[1,2], S Mancuso[3] and B Mazzolai[2,5]

[1] The BioRobotics Institute, Scuola Superiore Sant'Anna (SSSA), I-56025 Pontedera, PI, Italy
[2] Center for Micro-BioRobotics@SSSA, Istituto Italiano di Tecnologia (IIT), I-56025 Pontedera, PI, Italy
[3] Department of Plant, Soil & Environmental Science, University of Florence, I-50019 Sesto Fiorentino, FI, Italy

E-mail: barbara.mazzolai@iit.it

Abstract

The growth process of roots consists of many activities, such as exploring the soil volume, mining minerals, avoiding obstacles and taking up water to fulfil the plant's primary functions, that are performed differently, depending on environmental conditions. Root movements are strictly related to a root decision strategy, which helps plants to survive under stressful conditions by optimizing energy consumption. In this work, we present a novel image-analysis tool to study the kinematics of the root tip (apex), named *analyser for root tip tracks* (ARTT). The software implementation combines a segmentation algorithm with additional software imaging filters in order to realize a 2D tip detection. The resulting paths, or tracks, arise from the sampled tip positions through the acquired images during the growth. ARTT allows work with no markers and deals autonomously with new emerging root tips, as well as handling a massive number of data relying on minimum user interaction. Consequently, ARTT can be used for a wide range of applications and for the study of kinematics in different plant species. In particular, the study of the root growth and behaviour could lead to the definition of novel principles for the penetration and/or control paradigms for soil exploration and monitoring tasks. The software capabilities were demonstrated by experimental trials performed with *Zea mays* and *Oryza sativa*.

S Online supplementary data available from stacks.iop.org/BB/8/025004/mmedia

(Some figures may appear in colour only in the online journal)

1. Introduction

Plants, as sessile organisms, spend their entire lives at the site of seed germination. Consequently, they require a combination of plastic strategies to survive a variety of environmental conditions and stress-causing situations (Di Baccio *et al* 2009). Plants have evolved into organisms capable of surviving in continually changing environments. They are able to mine water and nutrients without having locomotion abilities. Their highly sensitive root tips, the apices, are constantly foraging while circumnavigating obstacles (Massa and Gilroy 2003a, 2003b), perceiving a myriad of external signals (Gilroy and Masson 2008), communicating with other plant tips (Bais *et al* 2003, Ciszak *et al* 2012). The root tip growth direction is a result of all these endogenous and exogenous factors. The decision making of growth direction is accomplished by roots without having a dedicated nervous system and this choice is crucial for plant survival. The understanding of root growth strategies could open up new horizons in different sectors and disciplines, including ICT technologies and robotics. New technologies could result from

---

[4] These authors contributed equally to this work.
[5] Author to whom any correspondence should be addressed.

the study of plant-root behaviour, such as the implementation of novel principles for soil penetration, energy-efficient actuation systems, sensory detection and distributed, adaptive control in networked structures with local information and communication capabilities. An example of a novel plant-root-inspired robotic system for soil exploration was recently presented by Mazzolai *et al* (2011).

The comprehension of plant-root behaviour goes hand in hand with the development of new tools that allow the observation of the root movements. Plants move a great deal, but they move on a different timescale from animals. There are different forms of movement in plants correlated with different behaviour. Many of the most interesting movements are related to plants' ability to develop specific growth responses (tropisms) to deal with their environment changes.

In the root apparatus, each single root has to move through the soil by orienting itself along the gravity vector, negotiating obstacles and locating resources. The apex of each root can sense many (more than ten) chemical and physical parameters from the surrounding environment, and it mediates the direction of root growth accordingly (Trewavas 2002, Fujita *et al* 2006, Di Baccio *et al* 2008, 2009). Light, gravity, oxygen, minerals and water availability vary in the soil both in direction and intensity, necessitating a continuously changing growth strategy for the roots. Root movements represent a first instance of active behaviour (Trewavas 2009), making the study of the *kinematics response* interesting for biological studies and necessary for the implementation of the behaviour in plant-root-inspired systems.

The kinematic analysis is based on the tracking of roots. In general, *tracking* refers to the action of following an object/feature over time and space. In this work, *tracking* refers to the action of following the path tracked over time by a recognizable part of the observed root system, the root tips. The term *tracking* should be distinguished from *tracing*, which indicates the action of extracting shape features of the observed root system (curvature, length, branching, etc), used by many root analysis tools, both academic (French *et al* 2008, 2009, Lobet *et al* 2011) and commercial (e.g., WinRHIZO, Regent Instruments, Montreal, QC, Canada).

The basic principles of kinematic analysis were first published by Darwin and Darwin (1880), who studied and described the movements of plants aroused by light, gravity and contact. These analyses relied on using an inclined glass plane, blackened with smoke, to evaluate the tropisms of plant roots. The marks left by growing roots on the smoked surface were photographed, qualitatively analysed and interpreted.

Since the Darwins' work, kinematic analysis has been successfully applied to the study of growth mechanisms, particularly those related to cell division and elongation (Beemster and Baskin 1998, Fiorani and Beemster 2006, Chavarría-Krauser *et al* 2007), and the ways stress conditions influence growth.

In this paper, we introduce a novel tool to study root tip kinematics for both primary and secondary roots, namely analyser for root tip tracks (ARTT), based on the analysis of images massively acquired. ARTT is a kinematic tracker, which automatically detects root tips, tracks root tip paths over time and specifies physical quantities, such as *trajectory*, *displacement*, *velocity*, *direction* and *orientation*. The acquired data are provided in a tabular or graphical form, helping to immediately and easily focus on the data of interest. No morphological and architectural analyses are performed by means of the proposed tool, which, conversely, focuses on tracking the root tip, the only part of the root that performs complex active movements (Sivagura and Horst 1998, Iijima *et al* 2008, Hahn *et al* 2008, Arnaud *et al* 2010, Baluška *et al* 2010). Moreover, in this study, the word 'kinematics' has a 'tip displacement kinematics' meaning, instead of 'growth kinematics'.

Some practical and simple case studies are introduced to show that ARTT does not imply strict experimental conditions (other than good separability between root system and background) when compared with other existing methods (e.g., acquisition system design, choice of the medium). Some experimental trials were performed on *Zea mays* and *Oryza sativa* species to demonstrate the features of the ARTT tool and its capabilities to work in environments in which growth conditions can be purposively changed over time by acting on stress factors (e.g., adding physical obstacles, chemicals, etc), which is of crucial relevance in the study of tropic responses of plant roots.

2. State of the art

Kinematic analysis regularly focuses on a massive collection of images. A number of tools (Armengaud *et al* 2009) provide an interactive approach by which the user recognizes and selects the points to track. This solution relies on the human ability to analyse images and recognize patterns, even within noisy images; at the same time, the highly subjective component makes results non-repeatable. Moreover, it is quite clear that the large number of data (usually hundreds of images) makes manual analyses both prohibitive and extremely prone to errors. These motivations lead to the development of solutions aimed at automating the process and minimizing user interaction.

Two of the best examples of root analysis tools are *KineRoot* (Basu *et al* 2007) and *RootTrace* (French *et al* 2008, 2009).

KineRoot provides a detailed analysis of plant growth kinematics focusing on the study of spatiotemporal patterns of growth and curvature of roots, also important for the study of gravitropic response. The tool uses particles of graphite as markers, which are used for the highest correlation pattern search. This technique works on square samples, applying a pattern-matching search and choosing for each image the samples with the highest correlation. The application of markers (ink- or carbon-derived particles) on the target plant region (Sharp *et al* 1988, Ishikawa *et al* 1991, Peters and Bernstein 1997, Basu *et al* 2007) simplifies the recognition step, but it is only suitable for short-range phenomena. In a long-range observation, the root system may evolve and produce new root tips, which cannot be marked in advance and consequently would not be tracked. In such situations, the
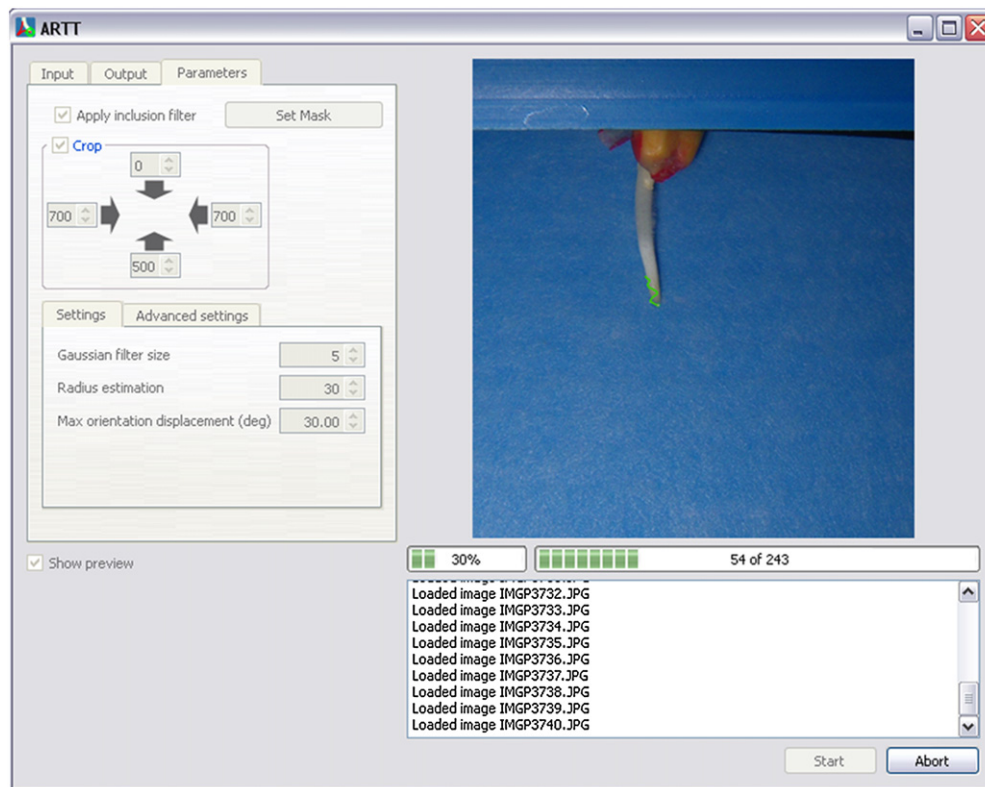
Figure 1. GUI of ARTT. ARTT generates over time a high-resolution track of the root tips appearing in an image sequence. The GUI allows tuning the parameters for automatic processing (pre-processing parameters, selection of the working area) through the tabs. A preview of the root tracking process is shown on the right side. The user has to indicate the source folder containing the images and can choose to process their subsequence. The output information can also be set up, indicating the desired format for the tabular output and if the graphical output is desired.

tool would provide a partial and incomplete view of the root system.

RootTrace is suitable for working on the primary root of Arabidopsis in order to study its gravitropic response over time. Even if the tool considers the temporal evolution, it is basically a tracer, meaning that the primary focus is on the detection of the root medial line, the evolution of which is analysed over time. Actually, it provides valuable results on thin roots and is able to trace the root growth in the downward direction because it focuses on gravitropic studies; on the other hand, this software does not allow the automatic recognition of new emerging root tips.

Recently, some studies on the three-dimensional (3D) reconstruction of plant-root architecture (Fang *et al* 2009, Clark *et al* 2011, Mairhofer *et al* 2012) have proposed a new way to observe roots and overcome the constraints of a two-dimensional (2D) growth space. A complete reconstruction suggests the ability to fully quantify the growth process. However, these studies focused on architectural and phenotypical analyses, and no kinematic information was provided.

3. Materials and methods

3.1. Implementation toolset

The ARTT software was implemented by using the C++ programming language. The graphical user interface

(GUI) (figure 1) is based on the *Qt* cross-platform graphic library (http://qt.nokia.com), while the processing backend, which involves image manipulation, is based on *OpenCV*, which is an open-source, cross-platform, computer vision and image-analysis library (http://opencv.willowgarage.com). OpenCV provides a set of built-in functions to handle images useful for root tip tracking, such as colour space conversion and channel extraction, a set of standard binarization algorithms, image histogram handling functions and noise filters. Moreover, it provides a low-level view of images, supporting and simplifying the development of new image handling algorithms.

3.2. Plant growth, setup and experimental methods

The ARTT software was validated by performing several experiments with maize (*Zea mays*) and rice (*Oryza sativa*) roots aimed at studying and tracking changes in roots over time.

A simple and effective setup was built to record the growth and movements of roots in a partially constrained 2D space for the described experiments (figure 2). The setup was built in order to work under different environmental conditions, for example, moving obstacles, adding different nutrients and using different kinds of growing medium or substrate. It consists of a plane that can slide through two side rails and two additional tracks for the positioning of the cameras. After
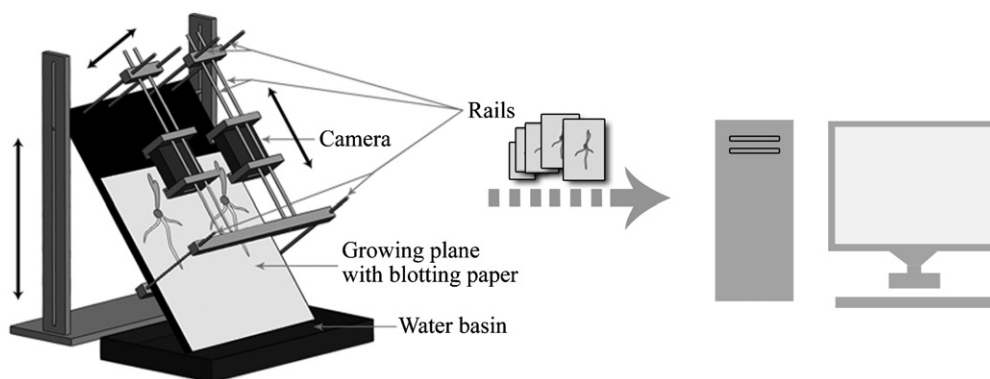
Figure 2. The experimental setup and the acquisition system. The experimental setup consists of a growth sliding plane and a support for the cameras. A sheet of blotting paper, coupled with a plastic blue panel, is placed on this plane. These items are jointly immersed into a basin filled with water and/or other substances. Seeds are placed and grown on this sheet of paper, which is kept wet by means of capillarity. Two cameras are placed parallel to the growth plane in their holding structures. This setup makes it possible among other things to act on the environment, dynamically changing the growth conditions. Alternatively, a Petri dish filled with gel (e.g., Phytagel™) can be used instead of blotting paper.

a short germination, seeds were transferred to a previously soaked sheet of 25 cm $\times$ 25 cm germination paper (*Bibby Filter Paper*) or a Petri dish with gel (i.e. 3 g of Phytagel™, Sigma-Aldrich Biotechnology LP, per 1 l of water), which was fixed on the setup plane. In the case that blotting paper was used as a growing medium, the underside of the plane was placed in a basin to allow direct contact with the nutrient solution.

The experiments were conducted in a closed cell for two to three days with regularly checked temperature (24–25 °C) and humidity (saturated).

Images were captured with high-resolution cameras (Pentax OPTIO W80 and W90) using the onboard interval shoot mode and shooting at 12 Mpx resolution. Exposure parameters were set in order to reduce the noise component (for flash-irradiated shots ISO 64, 28 mm equivalent focal length, f/4.2, 1/50 s; for external light irradiation ISO 100, 28 mm equivalent focal length, f/3.5, 1/4 s). For each experiment, a sprout (with radicles that are approximately long 2–4 cm for maize, and 0.5–1.5 cm for rice) was placed on the growth plane, situated at 10° from the plumb line, and its growth was observed for 10 h by referring to the time-lapse technique. Two different time-lapse frequencies, depending on the adopted spatial resolution, were used: acquisition period of 2 min with a spatial resolution of 25 μm px^{-1}, and 4 min with a spatial resolution of 40 μm px^{-1} for the experiments with moisture paper and Petri dishes with gel (Phytagel™, Sigma-Aldrich Biotechnology LP), respectively.

With the exception only of flash, when plants were grown on paper, the experiments were carried out in complete darkness to minimize root exposure to light, and the contrast between roots and background was increased by placing a plastic blue panel behind the paper. On the other hand, when plants were grown in a Petri dish with gel, the experiments were performed under continuous radiation with green light (Gilroy and Masson 2008) and images were taken without flash.

Even if working with Lab colour space makes the whole process more tolerant to non-homogeneous lighting

conditions, homogeneous and non-direct lighting is to be preferred, particularly for the detection of the thinnest secondary root tips. In the case that integrated flashes are used, the application of a scattering filter is strongly recommended, especially in closer acquisitions.

3.3. Tip detection

The tip detection capability of ARTT was tested on maize (*Zea mays*) roots grown on the blotting paper. The validation set consisted in 220 images containing 435 detections. Images were randomly chosen from 11 different image sequences with spatial resolution ranging between 15 and 76 μm px^{-1}, 20 random images per sequence.

Automatic detections were compared to manual detections on the original images and on pre-processed binarized images. The error measurement chosen for comparison was the chessboard distance in both cases because it best fits the discrete representation of images (see section 4.1.4 for a deeper explanation).

4. Results and discussion

4.1. The ARTT software

ARTT makes it possible to extract kinematic information on the movement of root tips (main and secondary roots) from a time-lapse sequence of images. Features extracted from images are mainly related to the tip paths with the goal of extracting information on the tropic nature of movements. The tool provides both a graphical output of tracks for immediate evaluation and a highly customizable textual output of features to be used in external statistical analyses. The entire quantification process consists of three main steps: (1) images go through an initial pre-processing phase, which produces a binary version of the images; (2) tip detection is subsequently applied to the binary images, mainly based on geometric features and without using any marker; (3) the last step incrementally builds up tracks by linking detections over time.

Table 1. Measured features. Schematic view of measured features for each tip detected and for each time step.

Features	Unit	Range	Description
Trajectory	(px, px)	([0; width], [0; height])	Tip position based on image coordinates.
Step displacement	px	–	Euclidean distance covered in a step.
Step velocity	px min^{-1}	–	Instantaneous velocity to cover each step (step displacement divided by acquisition time interval).
Step direction	Deg	[−180; 180]	Angle between step displacement direction and vertical direction. Negative values indicate moving to the left, positive values to the right.
Tip orientation	Deg	[−180; 180]	Angle between tip medial line and vertical direction. Negative values indicate orientation to the left, positive values to the right.

The main feature is the root tip *trajectory*, expressed as a sequence of positions over time. The trajectory only defines the path followed by root tips during their growth, and it does not necessarily match the final root system phenotype. Elaboration refers to the history of the tip movements associating the measured features of the root with the specific time lapse. Starting from the tip coordinates, the instantaneous linear *velocity* is calculated as the Euclidean distance between two following positions divided by the time lapse between two acquisitions. Velocity of tip displacement is also related to the growth rate (Yazdanbakhsh and Fisahn 2010) and is an important piece of information for studying stressful/favourable conditions. *Direction* is also provided as a step-by-step updated value. It is calculated as the angle between the line linking two following positions and the vertical direction. This parameter suggests the possibility of identifying, each time, the exact steering direction of the root tip. A feature not directly related to the trajectory but very useful for these studies is the root tip *orientation* (Mullen *et al* 1998, Vollsnes *et al* 2010), which is calculated as the angle between the terminal part of the medial line (calculated on a region three times as wide as the root diameter) and the vertical line on which the root tip lies. A schematic view of all the measured features is provided in table 1. The ability to define a tabular output with all the measured features for each root or a unique table for all the roots ordered by coming out-time is also provided. The former output is suitable for the single-root analysis, while the latter is particularly useful for correlating the simultaneous responses of two or more root tips to the same environmental state, extracting information regarding coordinated strategies.

The user can control a series of options, such as selecting the images that will be elaborated by ARTT, and reducing the computational cost by setting a crop region on the images and letting the software process only internal pixels. Performances can be improved using an inclusion filter that discards tip candidates placed outside a selected mask. This mask, drawn with a brush-like tool, increases its size during processing, thereby allowing detection of all the appearing root tips.

The user can also configure the desired output—graphical or textual (or both)—in a standard CSV format. If textual output is chosen, the user can express interest in a subset of recordable features or in a particular order. All this information can be easily customized, thus making it possible to achieve higher performance in both pre-processing (segmentation) and

processing (tip detection and root track building) phases. Finally, the user can manually refine results graphically relocating detected tips and correcting acquired data.

The whole processing time depends on the number and size of images, on the selected segmentation procedure and, to a lesser extent, on the number of detected tips. For example, a sequence of 700 2000 × 2500 sized images is processed in about 10 min using the triangle algorithm as a segmentation algorithm, while the hybrid thresholding algorithm can take up to three times more. Performances were tested on a modern Intel I5 processor. The performances could be improved by introducing some forms of parallelization in the heaviest calculations.

4.1.1. Pre-processing phase—segmentation. The core of the pre-processing step consists in the binarization of images (thresholding). The quality level depends strongly on the quality of the input images: the more the roots stand out from the background, the more accurate the threshold output will be. Roots are always assumed to be lighter than the background. Moreover, non-homogeneous lighting, shadows and reflections may compromise the output or introduce noise effects.

Many existing tools apply a channel selection to the RGB colour space to improve separability between background and foreground. In this colour range, each colour is created by combining three pure colours: red, green and blue. Depending on the tones, an image may look better contrasted on the component of one single colour. A common configuration consists of choosing a pure background with a tone well separated from the foreground and subsequently selecting the channel that offers better tone separability (typically, the red channel for a blue background). Since in RGB, colour space lighting information is distributed over all the channels, dealing with shadows and reflections is sometimes hard, especially with images acquired in white light. In these cases, better results are achieved working with colour spaces where lighting information is separated from tone information. In the *Lab* colour space, for example, information related to light only concerns channel *L*, whereas *a* and *b* channels show only information related to colour tonality (green–red and blue–yellow, respectively). Depending on the tonality of the background, images can still have low contrast, but regions preserve good separability. Using a blue background in the *b* channel, we will see a lighter root system on a darker
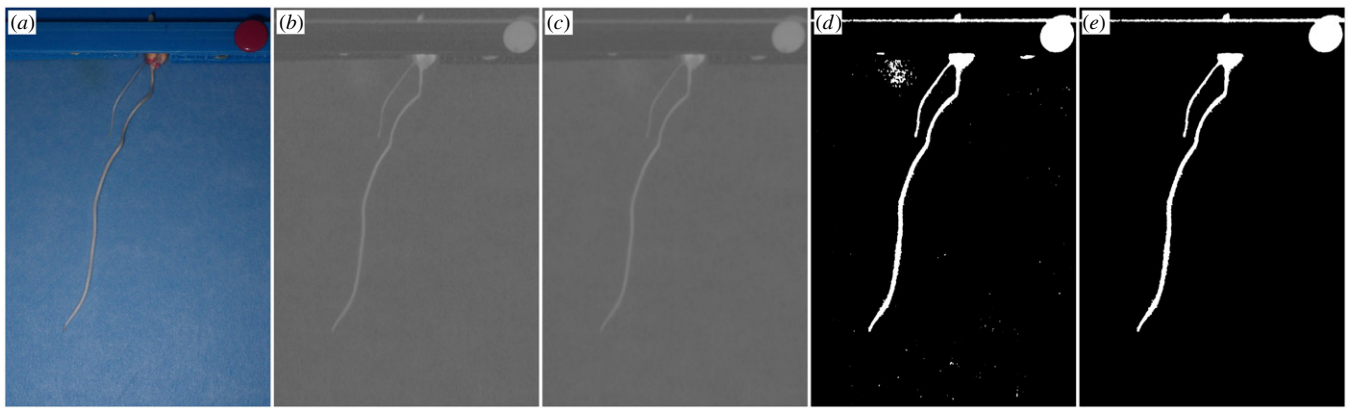
Figure 3. An example of the pre-processing steps applied to an image. (*a*) picture of the original image; (*b*) the channel *b* of the *Lab* colour space, extracted from image *A*; (*c*) application of a Gaussian filter; (*d*) a binary version of image *C*, obtained by applying the *triangle thresholding* method; (*e*) the final binary image, obtained by applying a cluster cleaning procedure to remove small noise artefacts.

background. This solution is useful under non-homogeneous light conditions and was provided in ARTT.

Because images can show slight lighting variations, we avoided referring to a fixed threshold value and chose an automatic method. Global binarization algorithms provide good results thanks to the appearance of only two main levels (background and roots). Among these algorithms, the triangle algorithm (Zack *et al* 1977) provides the best results because of the peculiar shape of the histogram of the handled image (see appendix). However, detecting the thinnest lateral roots still remains difficult, and the threshold chosen could split them up. To handle these cases, a hybrid solution was developed to combine the advantages of both local and global algorithms (see appendix).

The images then undergo Gaussian filtering to reduce noise and lossy compression artefacts. Once an image is represented in binary, a further noise filtering removes noisy patches due to thresholding. This filtering simply consists of scanning the foreground clusters in the image and removing all the clusters, based on an eight-neighbourhood connection, smaller than a user-defined threshold in the number of pixels. Figure 3 shows a complete sequence of pre-processing results.

4.1.2. Processing phase—tip detection. One of the main features of the ARTT software is the capability to self-recognize and track new roots with the aim to better understand behaviour and coordination strategies implemented by the root system. The software works with images taken using common cameras without any magnifier instrument and considers a root as a line, and the root tip its extremity. To better exploit this idea, we extracted the skeleton from the image through a thinning algorithm (Zhang and Suen 1984), thus achieving a good approximation of where root tips are, and applied a local search in that restricted area. The skeleton is always completely contained inside the contours of the roots; hence, given the skeleton of the image and a tip candidate, the tip location is calculated by the intersection of the skeleton (extended out of the edges) and the edges of the binarized root (figure 4). The distance between a tip of the skeleton and the relative edge increases with the thickness of the root, so the skeleton is
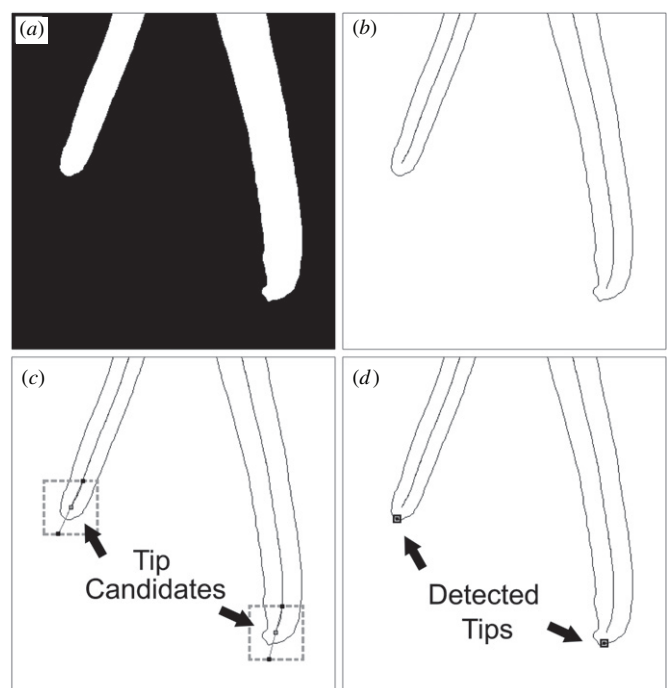

Figure 4. Root tips are extracted starting from the geometrical consideration that a root is a line. The roots are detected by calculating the root medial lines and extending them beyond the edge according to the linear direction of the terminal parts until an intersection is found. The area considered is contained in a square region centred on the tip candidate and three times wider than the tip diameter.

extended to the edge. Considering the square region centred on the tip candidate and three times wider than the root diameter (enough to ensure the intersection point is contained in it), the extension is a linear extension of the line between the centre (i.e. the tip candidate) and the point of the skeleton lying on the bounds of the square region. Other approaches can be adopted, but the common shape of root tips ensures this simple solution is accurate. Of course, the reliability of detection depends on the quality of the binary image. Thinning algorithms tend to preserve the morphology of the image, both for true details and for binarization artefacts.
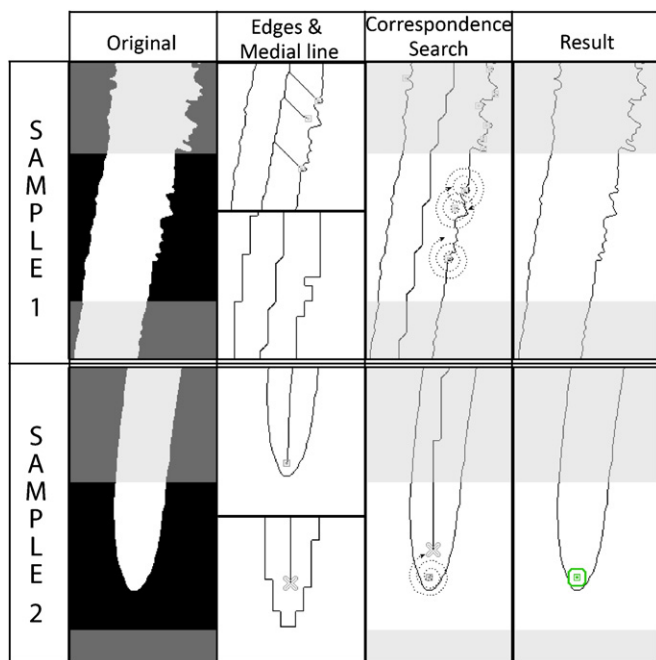
Figure 5. Tip candidates, the end points of medial lines, are filtered by checking their persistence in downsampled images. Downsampling introduces a loss of detail, which also means a loss of noise details for the binarization process. The spiral search, actually a square spiral search, is just a procedural way to implement a search for the nearest point satisfying the search criterion (in our case, terminal point of the skeleton) without any bias on the searching direction, minimizing the number of visited image pixels. Two samples are provided. For each sample, from left to right, the binarized image, the contours and medial line in the original size (above) and eight-time downsampled version (below), the search process around tip candidates for a downsampled counterpart and, finally, the result of filtering are shown. Only candidates in full resolution that show consistent (close and similarly oriented) candidates in the downsampled version are retained for further steps. In the first example, candidates are discarded; in the second one, the candidate is retained.

The detection is then refined through the application of a sequence of filters. The first filter is optional and refers to the user's discrimination skills; the user can define an inclusion mask on the image containing all the tips. This mask is used by the detection algorithm to filter out false positives (FPs). Since a request for user intervention for each image is not acceptable, the user has to fit the first image, including regions where a new root can appear; it is then up to the algorithm to evolve the mask according to the image sequence. Additionally, the mask can also be used to focus tracking only on a restricted set of tips.

Higher resolution provides more detail but also provides more potential artefacts. This consideration suggests one more filter: if a line (and the related line extremity) has no counterpart at a lower resolution image of a user-defined downsampling factor, the candidate is discarded (figure 5). Only tip candidates passing both the filters can be considered root tips. It is important to point out that this phase does not use any temporal information extracted from previous images. Each image is processed from scratch; in this way, elaboration is more expensive, but combined with the lack of markers, this

approach makes it possible to deal with new (secondary) root tips, thereby providing information on the whole root system's growth.

4.1.3. Processing phase—root track building. Each image processing produces a set of points. To build a track, a concatenation of points must be applied over time. When there is no more than one tip to track, the concatenation does not provide any issue. However, ARTT should be able to handle many tracks dynamically, starting a new track for each new root tip detected. In order to reach this target, two main issues have to be addressed: (1) how to correlate points of the same track over time, and (2) how to recognize new roots. To address the first issue effectively, we adopted a linear prediction. Given two consecutive points, we look for the next point moving in the same direction and distance as the previous point, analysing the surrounding area for the closest new point (figure 6).

It is possible that, because of temporary reflections, appearance of blobs, or mucilage secretion, the tip is missed in a few images. Without prediction, a subsequent detection would mislead to the creation of a new track, while the application of prediction over time is able to fill occasional gaps looking ahead for tips in a time-dependent location. Hence, for each registered tip location, the current location is considered for moving ahead, taking into account the time gap from its last occurrence.

Each new point that cannot be concatenated with the previous track is potentially the starting point for a new track. Nevertheless, in some cases, tip candidates that passed all the filters could be FPs. The last chance to recognize tip candidates as FPs and ignore them is to introduce a kind of *initial mistrust*: each candidate that cannot be concatenated with previous tracks starts a new track, but its track becomes effective only if new points are added in the following *n* time steps, where *n* is the mistrust factor set by the user. Even if it is possible to refine results in a postprocessing phase, this solution prevents discontinuous detections from altering track building by removing them and thus reducing the chances of unrelated point concatenation directly at the processing phase.

4.1.4. Evaluation of tip detection. The quality of the tracking results is closely related to the quality, namely the details and contrast, of the input images; however, the good results obtained at different resolutions suggest the suitability of the tool for a wide set of applications with different root species and different spatial resolutions.

The comparison of automatic detections versus manual detections on the original images using the chessboard distance (figure 7) as an error measurement showed an average error of 3.51 px (from 52.65 to 266.76 μm according to the image resolution; 87.75 μm at the most used resolution of 25 μm px^{-1}) and a standard deviation of 2.68 px (67.00 μm at 25 μm px^{-1}). The analysis of these results requires considering that the manual tip detection is often highly subjective and is sometimes non-repeatable because of shaded tip edges in images. Moreover, the release of mucilage tends to make detection even more difficult. Upon limiting the evaluation
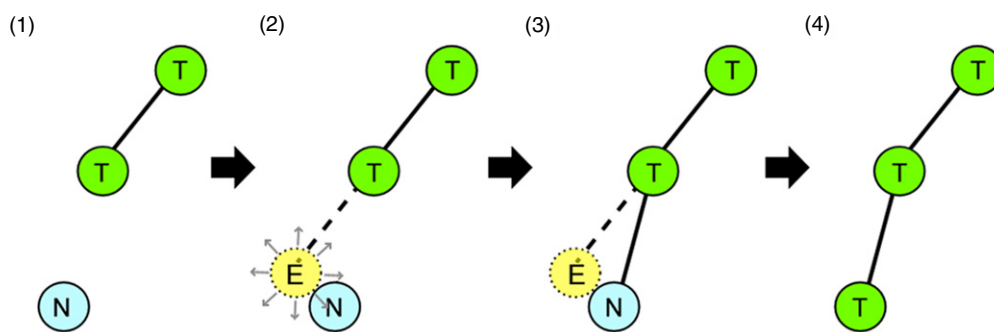
(1)　　　　　　　　　(2)　　　　　　　　　(3)　　　　　　　　　(4)

Figure 6. The correlation of each point is led by a linear prediction. Given an existing track, the next step is anticipated by repeating the previous step forward and starting a search for the closest point. The track points are marked with 'T', the new point with 'N' and the point expected with 'E'.
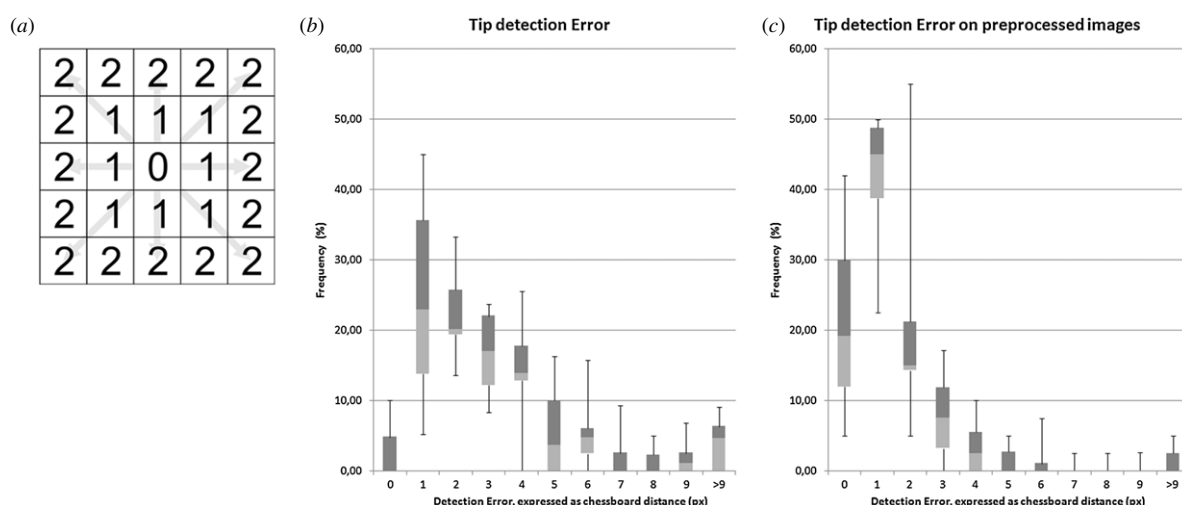

(*a*)　　　　　　(*b*) Tip detection Error　　　　　　(*c*) Tip detection Error on preprocessed images

Figure 7. The tip detection error is estimated as the Chebyshev distance between automatic detection and its related manual detection. The Chebyshev distance between two points in a 2D space is defined as the minimum difference along the two coordinates. This distance is also known as *chessboard distance* because, in a chess game, this distance represents the minimum distance in movement for a king to reach a square from its current one. It is particularly suitable for discrete spaces, as images, defined as 2D space of pixels, where a continuous metrics would not fit the space expressivity. (*a*) The table provides an intuitive representation of the chessboard distance. (*b*) and (*c*) The charts show the distribution of tip detection error over a set of 11 different acquisition sequences. (*b*) The chart shows automatic detection compared with manual detection over original images. (*c*) The chart shows manual detection performed over previously binarized images through pre-processing. The shaped edges of binary images reduce the subjective component of manual detection and results are closer.

to sequences acquired in the best conditions (well-contrasted images, no mucilage blobs), the error improves to an average value of 1.77 px (from 26.55 to 134.52 μm according to the image resolution; 44.25 μm at 25 μm px^{-1}) with a standard deviation of 1.18 px (29.50 μm at 25 μm px^{-1}) over a set of 105 detections.

To restrict the evaluation only to the tip detection procedure, the same evaluation (comparison between automatic and manual detections) was performed on pre-processed images. In this case, manual detections worked on binary well-bounded images; therefore, manual detections are more easily repeatable, and any difference in the detection is caused by a divergence in the automatic procedure. As expected, the error is reduced with an average value of 1.63 px (40.75 μm at 25 μm px^{-1}) and a standard deviation of 1.79 px (44.75 μm at 25 μm px^{-1}). A box plot of these results is shown in figure 7.

We found that the main issue is root colour and transparency, more than root thickness. This feature is the

reason for the difficult detection at lower resolutions for some lateral roots.

Another issue worth noting is the tip missing mainly due to the binarization process. Thanks to predictions during the track-building step, isolated misses are recovered, whereas repeated misses may produce split and useless tracks.

4.2. Root tip kinematics: root growth and nutation analysis

The ARTT software can be used to investigate tip displacement kinematics due to growth and nutations. This type of study is important because nutation movements, also called circumnutations (CNs), result from asymmetrical growth and have mainly endogenous nature, with their parameters (i.e. period and amplitude of nutation) that may be influenced by gravity, touch and chemical stimuli (Hirota 1980, Brown 1991, 1993, Shabala and Newman 1997, Migliaccio *et al* 2009). They were found to be correlated with anchorage capabilities of rice roots in flooded soil (Inoue *et al* 1999), and are believed to
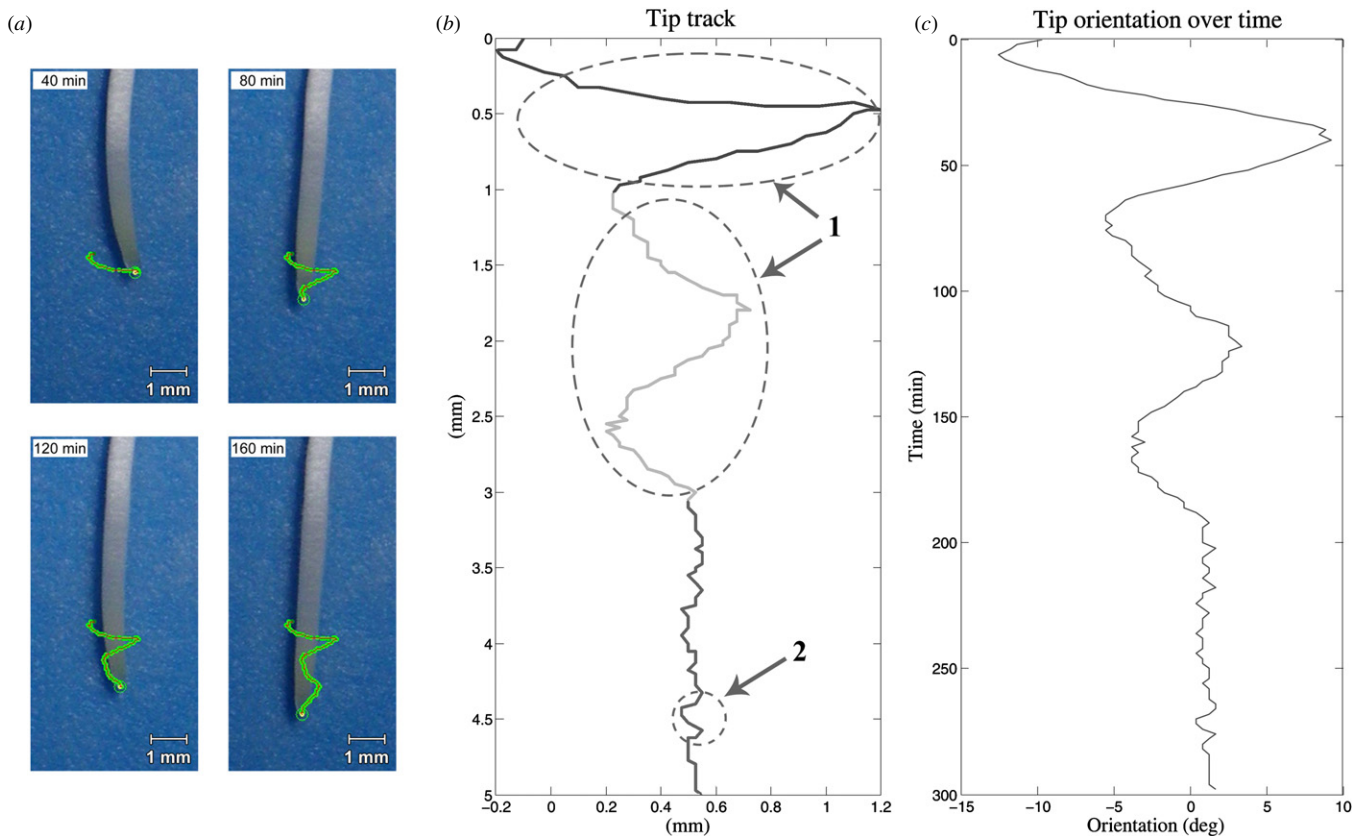
(*a*)

(*b*) Tip track

(*c*) Tip orientation over time

Figure 8. Quantitative results extracted from the track of a maize root. (*a*) The sequence shows the path followed by the root tip (time intervals of 2 min). (*b*) A detailed view of the tip track is provided. The pendulum movements, or lateral fluctuations of the root tip, with two different amplitudes and periods are indicated with number 1, whereas fast, small amplitude lateral displacements are indicated with number 2. The quasi-rectilinear growth is observable from 3 mm in vertical displacement. (*c*) The tip orientation over time is shown.

contribute to root soil penetration by displacing soil on both sides, as the root apex pushes itself through the medium (Hirota 1976, 1980, Vollsnes *et al* 2010). The variations in a growth pattern may have an endogenous nature or be linked to external causes (Hirota 1980, Brown 1991, Shabala and Newman 1997, Migliaccio *et al* 2009).

ARTT was successfully used to track CN movements of *Zea mays* and *Oryza sativa* roots (see supplementary materials—videos 1 and 2, available from http://stacks.iop.org/BB/8/025004/mmedia) grown on paper and Phytagel™ substrates. Figure 8(*a*) shows a representative growth pattern for the described experiments performed on the setup with the moisture paper. This growth pattern accurately reflects the movements performed by the primary root: (i) two initial lateral oscillations of 64 min duration and 0.7 mm amplitude (0–1 mm in vertical displacement, figure 8(*b*)), (ii) three consecutive lateral oscillations with an amplitude of about 0.25 mm and period of about 60–100 min (1–3 mm in vertical displacement, figure 8(*b*)) and (iii) a quasi-rectilinear growth (from 3 mm in vertical displacement, figure 8(*b*)). The fast oscillation movements of a period approximately 4–16 min, which were observed in the time-lapse video, were also detected in the tip track (indicated by number 2 in figure 8(*b*)).

Extracted data may be used, for example, to estimate the growth rate from the tip displacement velocity (Yazdanbakhsh and Fisahn 2010), to calculate the CN period from orientation angles (figure 8(*c*): Mullen *et al* (1998)), as well as to find

the CN amplitudes and periods from tip tracks (figure 8(*b*): Popova *et al* (2012)).

4.3. Root tip kinematics: obstacle avoidance

The obstacle avoidance tropism is the capacity of roots to circumnavigate the obstacles or patches of extremely compact soil. Obstacle avoidance is one of the most important tropisms affecting root growth and its function is strictly related to touch sensing. This section describes how ARTT can be used to study the variation of orientation during root obstacle avoidance in maize roots.

There are different physical stimuli linked with mechano-response in a plant root. Among others, haptotropism refers to the constant contact with an object, generating a constant pressure on the plant cells or, simply, touch. For a complete review on terms and definition, see Mitchell and Myers (2010).

Massa and Gilroy (2003a, 2003b) studied in depth phenomena related to obstacle avoidance in *Arabidopsis thaliana*. They found that the ability of roots to avoid and overcome obstacles dynamically changing the tip orientation can be described by some key parameters (Gilroy and Masson 2008), which can be shortly described as follows.

– The gravitropic set point angle (GSA), the angle that the apex assumes while penetrating the soil. This angle is very important since it contributes to the root architecture
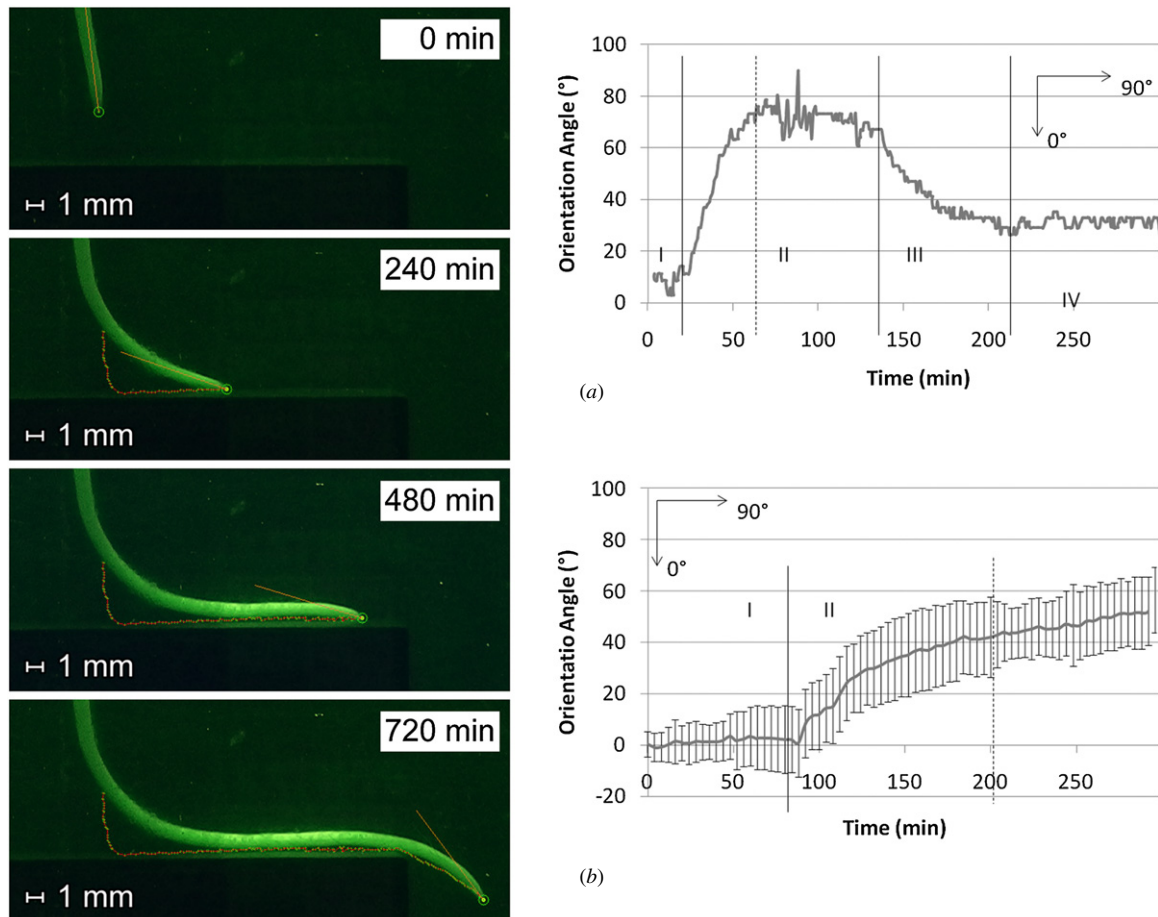
Figure 9. The root tip orientation angle during the obstacle avoidance tropism: (*a*) the trend for a representative example, (*b*) the average trend for nine experimental trials; vertical bars indicate the standard deviation. The plots are divided into several phases: I—the approaching phase before contact with a flat obstacle; II—the phase during the obstacle crossing with tip in contact with the obstacle; III—the recovery phase after the obstacle circumnavigation; IV—growth after the recovery phase. In phase II, a transition region, delimited by a dashed line, may be observed before the orientation angle becomes steady. The transition stage before the stabilization of orientation angle was observed to last from 1–2 h.

which, in turn, determines their efficiency in acquiring soil resources.

– The root tip-to-barrier angle during the touch phase (obstacle crossing or circumnavigation). In our study, the tip-to-obstacle angle during the crossing phase is equal to 90° minus the orientation angle, the obstacle being positioned horizontally.

– Root recovery angle after the obstacle circumnavigation.

A study similar to the work proposed by Gilroy and Masson (2008) was here performed with primary maize roots in order to demonstrate how ARTT can detect obstacle avoidance behaviour in roots. In this kind of study, ARTT offers the advantage of automatically tracing and calculating the tip orientation angle with respect to the plumb line.

A maize root was grown inside a Phytagel^TM substrate (3 g per 1 l of water) in a Petri dish, in which a flat obstacle was previously positioned. The root growth was observed and recorded for two days by means of the setup described in section 3.2, with a time-lapse period of 4 min.

An example of variation in tip orientation during the obstacle avoidance tropism is shown in figure 9(*a*) (see also supplementary materials—video 3, available from

http://stacks.iop.org/BB/8/025004/mmedia). Four different regions may be distinguished from the plot: (1) the approaching phase before the root tip contacts the obstacle; (2) the crossing phase during the obstacle circumnavigation; (3) the recovery phase after the obstacle circumnavigation; (4) the region of growth after the recovery phase. The orientation angle was observed to be less than 20° in the approaching phase, which is coherent with the GSA in maize roots (Firn and Digby 1997). The orientation angle was stabilized at approximately 70° during the crossing phase. Finally, when the obstacle was overcome, the tip resets its set point angle with respect to the touch-driven phase. The resulting was orientation angle after the recovery phase higher with respect to the initial GSA (approximately 30° after 2 h of recovery phase). The recovery phenomenon was observed to be different from the obstacle avoidance in *Arabidopsis thaliana*, probably because of the plagiotropic nature of maize roots that is different from the gravitropic behaviour in *Arabidopsis thaliana* roots (Leopold and Wettlaufer 1989, Firn and Digby 1997, Gilroy and Masson 2008). Figure 9(*b*) shows the mean angle and its standard deviation during the obstacle avoidance for nine maize roots. The results are similar to the outcomes
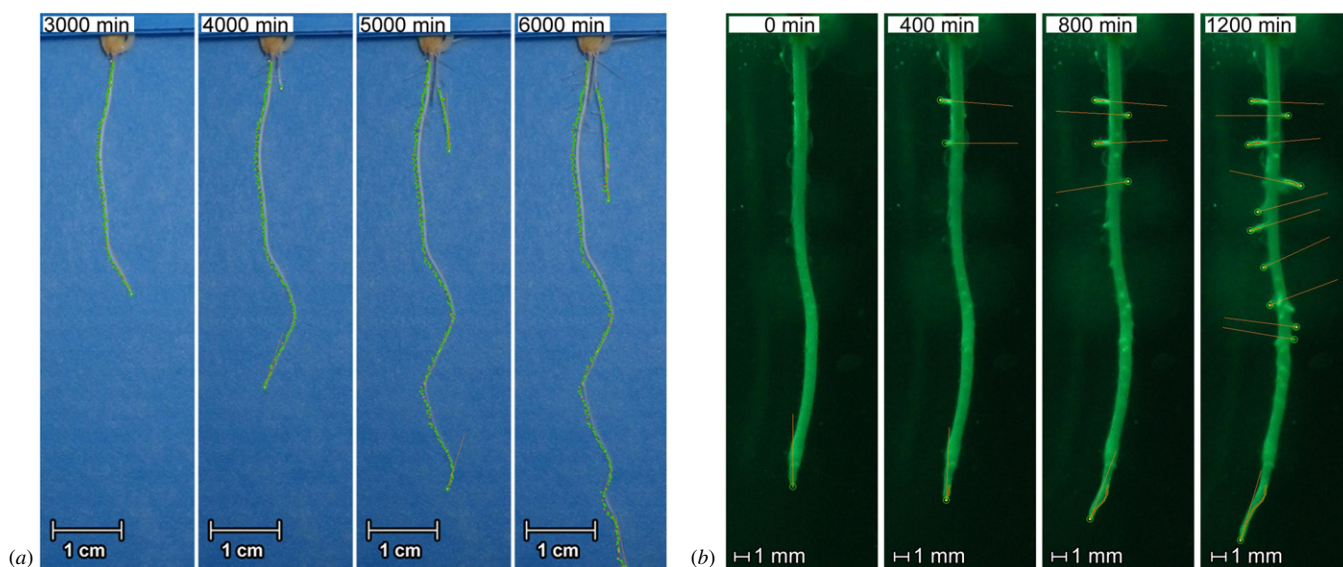
Figure 10. Examples of tracking of a rice root on blotting paper (*a*) and of a maize root in a Phytagel™ substrate (*b*). Although rice roots are thinner than maize roots, the tool correctly tracked them. This tool also showed the ability to detect and track second roots automatically. (*b*) A few secondary roots could not be detected because they showed low contrast with the background.

Table 2. The statistics of root tip orientation angle during the obstacle avoidance tropism in the primary maize root with a flat obstacle. The 88 min before the tip contact with the obstacle were considered the approaching phase. The values of the crossing and recovery phases were taken after the transition stage of 120 min. The n/d (not defined) indicates trials with missing data of growth after the recovery phase, because the trials were not long enough. Values express the orientation angle of the root tip with respect to the vertical direction, in a counterclockwise representation.

	Approaching phase (for 88 min)		Crossing phase (after 120 min transition stage)		Growth after the recovery phase (for 120 min)	
	Average (deg)	Standard deviation (deg)	Average (deg)	Standard deviation (deg)	Average (deg)	Standard deviation (deg)
Trial 1	− 5.77	2.89	72.89	9.76	67.27	3.02
Trial 2	− 2.41	1.19	78.53	9.27	61.18	2.16
Trial 3	5.45	5.18	65.82	5.32	42.13	2.96
Trial 4	− 7.47	1.21	35.45	2.55	n/d	n/d
Trial 5	16.49	3.70	54.42	7.10	n/d	n/d
Trial 6	2.49	2.33	31.52	8.53	n/d	n/d
Trial 7	3.74	2.33	67.17	11.32	n/d	n/d
Trial 8	− 8.52	1.69	64.84	12.89	5.49	8.40
Trial 9	5.45	5.18	65.82	5.32	42.13	2.96

presented by Massa and Gilroy (2003a) regarding the general behaviour of the tip. In table 2, average and deviation standard of tip orientation angle are listed for each trial during the approaching phase, the crossing phase after the transition stage and the final angle after the recovery phase.

4.4. Secondary root handling

One of the peculiarities concerning the proposed tool involves the ability to detect automatically the outcoming secondary roots. The analysis of the whole root system makes it possible to investigate the global strategy adopted under different environmental conditions with the possibility of comparing the role and functionality of each single root, one with the other. The basic idea is that a simultaneous comparative analysis of single-root tips, in terms of position, velocity and orientation, with the knowledge available in the environment, can be useful to infer the energy optimization strategy. In this way,

we can observe and quantify, for example, the influence of nutrient concentration in a spot area in the velocities of all the tips. Figure 10 shows a number of testing experiments (see also supplementary materials—videos 3 and 4, available from http://stacks.iop.org/BB/8/025004/mmedia), with new roots being detected and tracked over time after they come out in the image.

5. Conclusions

The development of innovative tools for the automatic root analysis is attracting more and more effort, because they allow enhancements in accuracy and versatility and reduction in time. Computer-aided analyses are becoming popular in phenotypic and in physiological studies. The presented ARTT tool allows us to study the kinematics of plant-root apices related to growth and tropic responses. The study of root tip

kinematics includes the analysis of tip displacement and its data can be used to assess growth velocity (Yazdanbakhsh and Fisahn 2010), as well as circumnutation detection and quantification of its period (Mullen *et al* 1998, Popova *et al* 2012). Moreover, ARTT allows us to recognize multiple root tips and this feature is notably useful to study the root apparatus structure, to investigate the roots decision strategy and the relationships among single roots. Accordingly, ARTT holds out two main applications: on the one hand, the development of this new investigation tool can be useful to develop models and testable hypotheses of partly unknown aspects of plant roots, such as principles of adaptive growth, and collective behaviour; on the other hand, the studied plant-root efficient strategies can be applied to develop a new generation of ICT solutions and root-inspired robotic systems for tasks of soil exploration and monitoring (Mazzolai *et al* 2011). Moreover, solutions for releasing the software in a distribution form and consequently increasing its application fields are under investigation. ARTT was validated with some experimental trails of tip kinematics analysis and handling of multiple tip detection. Preliminary results on obstacle avoidance tropism are reported, and they demonstrated the ability of the software to automatically and precisely describe the kinematics of root growth. From a biological point of view, the challenge and the innovation of this study lie in increasing knowledge on how the root system architecture and behaviour are influenced by the environment. This work essentially proposes a tool to investigate the way external stimuli (natural and/or stress factors) affect the development of the roots (i.e. kinematics parameters). This perspective to collect data by means of ARTT and analyse them hereafter guides the researcher to a better comprehension of the principles that allow plants to explore soil in an efficient way. Furthermore, studies on the ability that roots show in coordinating apices for the optimization of nutrient uptake (Buchner *et al* 2004), on their extremely modular nature and their sensing capabilities arranged in the root tips (Arnaud *et al* 2010, Kiss 2006) permit investigation of the root growth in terms of 'self-organized and emerging adaptive behaviour' (Ciszak *et al* 2012), which represents an interesting paradigm to develop new control rules for new robotic systems, able to autonomously adapt to unexpected conditions, as demonstrated by the biological counterpart.

Acknowledgment

Appendix

A.1. Global thresholding

Thresholding algorithms obtain greyscale images and provide their two-colour (black and white) version. With a particular focus on typical images considered for the analysis, the
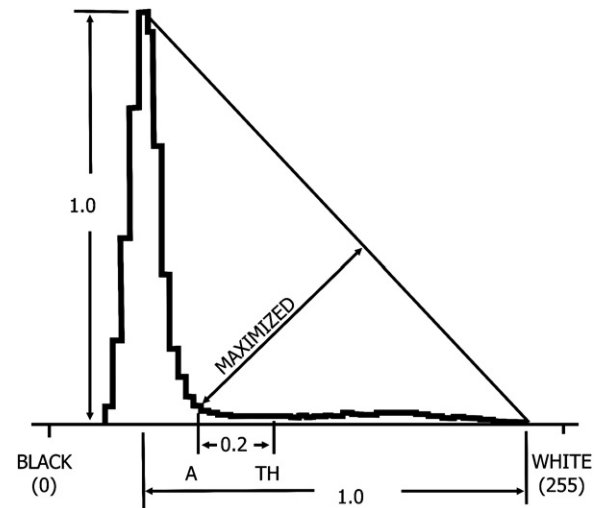

Figure A1. Determination of the global threshold with the triangle algorithm. The threshold (TH) was selected by normalizing the height and dynamic range of the intensity histogram, locating point A as shown and then adding a fixed offset. Image modified from Zack *et al* (1977).

adoption of a uniform or nearly uniform background guarantees the applicability of a global binarization algorithm with good results. The widely adopted Otsu algorithm (Otsu 1979) assumes a bimodal histogram shape and calculates the threshold value that minimizes the intra-class variance. In the cases of non-bimodal histograms, however, results could be far from those expected. An algorithm that works well on a completely different histogram shape is the triangle algorithm (Zack *et al* 1977). It assumes a histogram shape characterized by a peak ending with a long low tail. The algorithm calculates, hence, the line linking the extreme level (in our case, the lightest) with the peak value and looking for the level whose value maximizes the distance from the calculated line (figure A1). The images we have to deal with are often multimodal, but in any case, our purpose is to distinguish roots, which are light and occupy a relatively small portion of the whole image, from the rest. The common histogram shape we observe provides a long low tail in the highest (lightest) region of the histogram, and this is because the triangle algorithm turns out to be much more suitable than the more common Otsu algorithm for our purposes.

A.2. Hybrid thresholding algorithm

With a global algorithm, the detection of the thinnest lateral roots still remains difficult, and the threshold chosen could split them up. On the other hand, local methods tend to enhance details that are meaningless. The attempt to mix together the advantages of both global and local approaches leads to a hybrid solution more suitable for our purposes.

The binarization phase starts with a first application of a triangle algorithm, modified to be more robust in multimodal histograms, which provides a global guide threshold. The image is then split into partially overlapped square subsamples, which are processed locally, depending on certain relevant statistics (e.g., maximum and minimum values, histogram
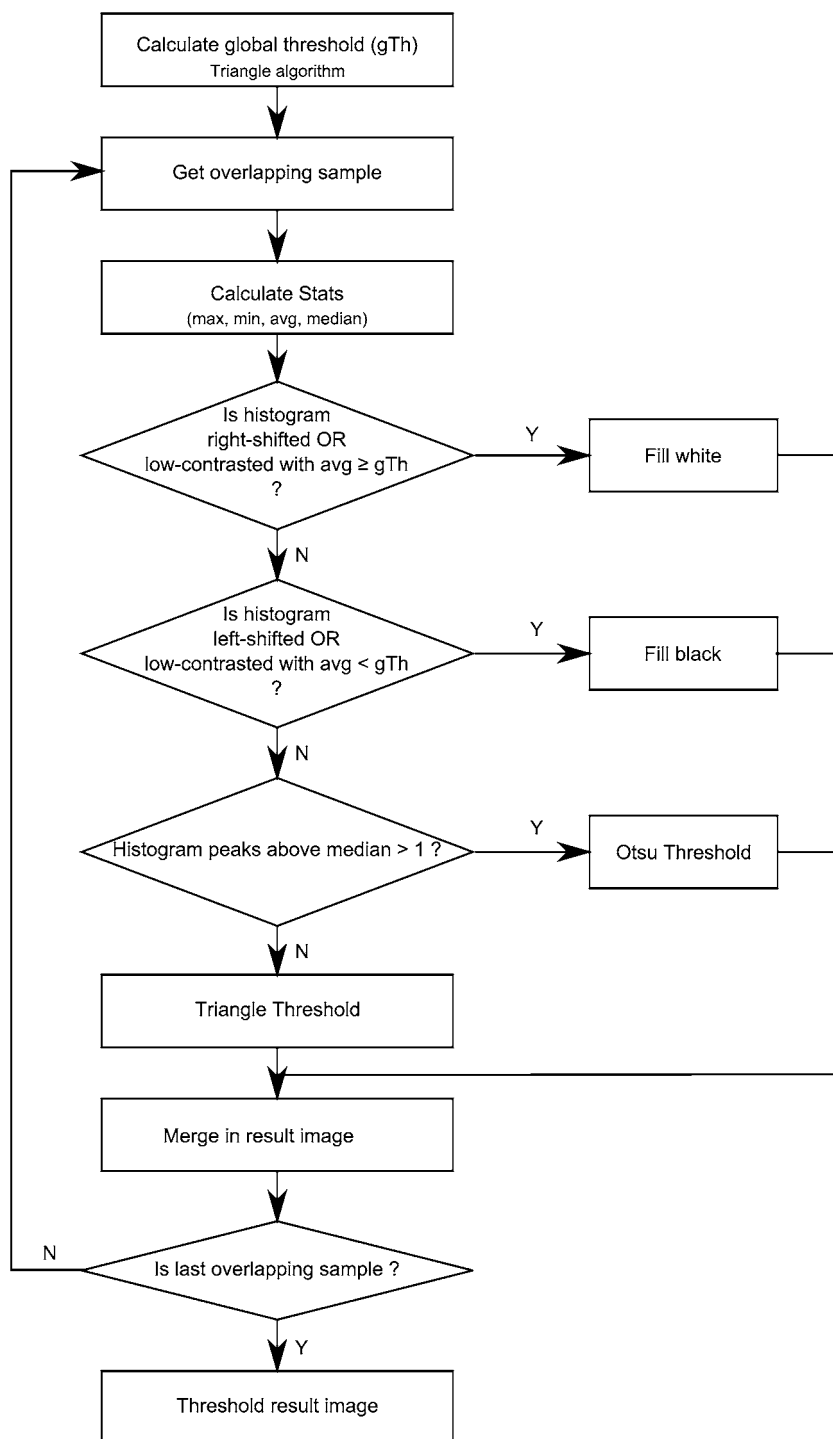
Figure A2. Flowchart of the automatic hybrid thresholding method used in the pre-processing phase. A global threshold calculated by the application of the triangle algorithm is used as a guideline for the local threshold of overlapping samples. If the sample histogram is completely shifted compared to the global threshold or if the image is poorly contrasted, then the sample is uniformly filled based on its average. Otherwise, the sample is thresholded according to the histogram shape, choosing between the Otsu and triangle methods. The final result will take into account the result of each overlap.

position compared with the global guide threshold, dynamic range), by applying Otsu thresholding, triangle thresholding, or simply uniformly filling it. A greyscale image is then built up averaging the values among overlapped processed samples. A final threshold phase cuts off all the patches that do not reach a confidence of 70%. A detailed flowchart of the algorithm is shown in figure A2. The square samples are sized to 2.5 times the average root diameter. This choice guarantees a good trade-off between advantages of both global and local thresholding methods. The overlapping factor, instead, is user defined. An overlapping factor of 3 usually provides good results limiting time consumption. Processing overlapped samples makes the

algorithm computationally more expensive, but this problem is outside our purposes, as it will proceed offline and without user interaction.

References

Armengaud P, Zambaux K, Hills A, Sulpice R, Pattison R J, Blatt M R and Amtmann A 2009 EZ-Rhizo: integrated software for the fast and accurate measurement of root system architecture *Plant J.* **57** 945–56

Arnaud C, Bonnot C, Desnos T and Nussaume L 2010 The root cap at the forefront *C. R. Biologies* **333** 335–43

Bais H P, Vepachedu R, Gilroy S, Callaway R M and Vivanco J M 2003 Allelopathy and exotic plant invasion: from molecules and genes to species interactions *Science* **301** 1377–80

Baluška F, Mancuso S, Volkmann D and Barlow P W 2010 Root apex transition zone: a signalling response nexus in the root *Trends Plant Sci.* **15** 402–8

Basu P, Pal A, Lynch J P and Brown K M 2007 A novel image-analysis technique for kinematic study of growth and curvature *Plant Physiol.* **145** 305–16

Beemster G T S and Baskin T I 1998 Analysis of cell division and elongation underlying the developmental acceleration of root growth in Arabidopsis thaliana *Plant Physiol.* **116** 1515–26

Brown A H 1991 Gravity perception and circumnutation in plants *Adv. Space Biol. Med.* **1** 129–53

Brown A H 1993 Circumnutations: from Darwin to space flights *Plant Physiol.* **101** 345–8

Buchner P, Takahashi H and Hawkesford M J 2004 Plant sulphate transporters: co-ordination of uptake, intracellular and long-distance transport *J. Exp. Bot.* **55** 1765–73

Chavarría-Krauser A, Nagel K A, Palme K, Schurr U, Walter A and Scharr H 2007 Spatio-temporal quantification of differential growth processes in root growth zones based on a novel combination of image sequence processing and refined concepts describing curvature production *New Phytol.* **177** 811–21

Ciszak M, Comparini D, Mazzolai B, Baluska F, Arecchi F T, Vicsek T and Mancuso S 2012 Swarming behavior in plant roots *PLoS ONE* **7** e29759

Clark R T, MacCurdy R B, Jung J K, Shaff J E, McCouch S R, Aneshansley D J and Kochian L V 2011 Three-dimensional root phenotyping with a novel imaging and software platform *Plant Physiol.* **156** 455–65

Darwin C and Darwin F 1880 *The Power of Movement in Plants* (London: John Murray)

Di Baccio D, Castagna A, Paoletti E, Sebastiani L and Ranieri A 2008 Could the differences in O3 sensitivity between two poplar clones be related to a difference in antioxidant defense and secondary metabolic response to O3 influx? *Tree Physiol.* **28** 1761–72

Di Baccio D, Tognetti R, Minnocci A and Sebastiani L 2009 Responses of the Populus × euramericana clone I-214 to excess zinc: carbon assimilation, structural modifications, metal distribution and cellular localization *Environ. Exp. Bot.* **67** 153–63

Fang S, Yan X and Liao H 2009 3D reconstruction and dynamic modeling of root architecture *in situ* and its application to crop phosphorus research *Plant J.* **60** 1096–108

Fiorani F and Beemster G T S 2006 Quantitative analyses of cell division in plants *Plant Mol. Biol.* **60** 963–79

Firn R D and Digby J 1997 Solving the puzzle of gravitropism—has a lost piece been found? *Planta* **203** S159–63

French A P, Bennett M J, Howells C, Patel D and Pridmore T 2008 A probabilistic tracking approach to root measurement in images *BIOSIGNALS 2008: Proc. 1st Int. Conf. on Biomedical Electronics and Devices* ed P Encarnação and A Veloso pp 108–15

French A P, Ubeda-Tomás S, Holman T J, Bennett M J and Pridmore T 2009 High-throughput quantification of root growth using a novel image-analysis tool *Plant Physiol* **150** 1784–95

Fujita K, Matsuyama A, Kobayashi Y and Iwahashi H 2006 The genome-wide screening of yeast deletion mutant to identify the genes required for tolerance to ethanol and other alcohols *FEMS Yeast Res.* **6** 744–50

Gilroy S and Masson P H 2008 Front matter *Plant Tropisms* 1st edn (Oxford: Blackwell)

Hahn A, Zimmermann R, Wanke D, Harter K and Edelmann H G 2008 The root cap determines ethylene-dependent growth and development in maize roots *Mol. Plant* **1** 359–67

Hirota H 1976 Rotation growth of root tips in Zea mays and lolium multiflorum *J. Japan. Soc. Grassl. Sci.* **22** 156–60

Hirota H 1980 Endogenous factors affecting the curved growth of seminal roots of *Zea mays* L. seedlings grown in liquid culture *Plant Cell Physiol.* **21** 961–8

Iijima M, Morita S and Barlow P W 2008 Structure and function of the root cap *Plant Prod. Sci.* **11** 17–27

Inoue N, Arase T, Hagiwara M, Amano T, Hayashi T and Ikeda R 1999 Ecological significance of root tip rotation for seedling establishment of Oryza sativa L *Ecol. Res.* **14** 31–38

Ishikawa H, Hasenstein K H and Evans M L 1991 Computer-based video digitizer analysis of surface extension in maize roots *Planta* **183** 381–90

Kiss J Z 2006 Up, down, and all around: how plants sense and respond to environmental stimuli *Proc. Natl Acad. Sci. USA* **103** 829–30

Leopold A C and Wettlaufer S H 1989 Springback in root gravitropism *Plant Physiol.* **91** 1247–50

Lobet G, Pagès L and Draye X 2011 A novel image-analysis toolbox enabling quantitative analysis of root system architecture *Plant Physiol.* **157** 29–39

Mairhofer S, Zappala S, Tracy S R, Sturrock C, Bennett M, Mooney S J and Pridmore T 2012 RooTrak: automated recovery of three-dimensional plant root architecture in soil from x-ray microcomputed tomography images using visual tracking *Plant Physiol.* **158** 561–9

Massa G D and Gilroy S 2003a Touch modulates gravity sensing to regulate the growth of primary roots of Arabidopsis thaliana *Plant J.* **33** 435–45

Massa G D and Gilroy S 2003b Touch and gravitropic set-point angle interact to modulate growth in roots *Adv. Space Res.* **31** 2195–202

Mazzolai B, Mondini A, Corradi P, Laschi C, Mattoli V, Sinibaldi E and Dario P 2011 A miniaturized mechatronic system inspired by plant roots for soil exploration *IEEE/ASME Trans. Mechatronics* **16** 201–12

Migliaccio F, Fortunati A and Tassone P 2009 Arabidopsis root growth movements and their symmetry: Progress and problems arising from recent work *Plant Signaling Behav.* **4** 183–90

Mitchell C A and Myers P N 2010 Mechanical stress regulation of plant growth and development *Horticultural Reviews* vol 17 (New York: Wiley) pp 1–42

Mullen J L, Turk E, Johnson K, Wolverton C, Ishikawa H, Simmons C, Söll D and Evans M L 1998 Roles of gravitropism and circumnutation in the waving/coiling phenomenon *Plant Physiol.* **118** 1139–45

Otsu N 1979 A threshold selection method from gray-level histograms *IEEE Trans. Syst. Man Cybern.* **9** 62–66

Peters W S and Bernstein N 1997 The determination of relative elemental growth rate profiles from segmental growth rate profiles from segmental growth rates *Plant Physiol.* **121** 905–12

Popova L, Russino A, Ascrizzi A and Mazzolai B 2012 Analysis of movement in primary maize roots *Biologia* **67** 517–24

Shabala S N and Newman I A 1997 Proton and calcium flux oscillation in the elongation region correlate with root nutation *Physiol. Plant.* **100** 917–26

Sharp R E, Silk W K and Hsaio T C 1988 Growth of maize primary root at low water potentials: 1. Spatial distribution of expansive growth *Plant Physiol.* **87** 50–57

Sivagura M and Horst W J 1998 The distal part of the transition zone is the most aluminum-sensitive apical root zone of maize *Plant Physiol.* **116** 155–63

Trewavas A 2002 Mindless mastery *Nature* **415** 841

Trewavas A 2009 What is plant behaviour? *Plant Cell Environ.* **32** 606–16

Vollsnes A V, Futsaether C M and Bengough A G 2010 Quantifying rhizosphere particle movement around mutant maize roots using time-lapse imaging and particle image velocimetry *Eur. J. Soil Sci.* **61** 926–39

Yazdanbakhsh N and Fisahn J 2010 Analysis of Arabidopsis thaliana root growth kinetics with high temporal and spatial resolution *Ann. Bot.* **105** 783–91

Zack G W, Rogers W E and Latt S A 1977 Automatic measurement of sister chromatid exchange frequency *J. Histochem. Cytochem.* **25** 741–53

Zhang T Y and Suen C Y 1984 A fast parallel algorithm for thinning digital patterns *Commun. ACM* **27** 236–9